

in the vicinity of T_c [Fig. 2(c)]:

$$k^{-2} \equiv \chi_{22}^X / (\chi_{22}^X - \chi_{22}^x) = A(T - T_0), \quad (16)$$

$$(d_{25}a_{25})^{-1} \equiv \chi_{22}^x / (\chi_{22}^X - \chi_{22}^x) = A(T - T_c). \quad (17)$$

From the free energy F [Eq. (1)], the relations

$$k^{-2} = C^P(\chi^x)^{-1}/a^2, \quad (18)$$

$$(da)^{-1} = C^P(\chi^x)^{-1}/a^2 = C^E(\chi^x)^{-1}/a^2, \quad (19)$$

are derived. In both cases I and II, k^2 and da diverge (Fig. 1). Therefore, the experimental results (16) and (17) provide strong support that LAT is described by the free energy F_2 [Eq. (3)]. Furthermore, the temperature dependence of χ^x , χ^x , C^E , and C^P clearly shows that LAT belongs to case II.

So far many crystals have been reported to undergo the transition at which the elastic stiffness vanishes. In some crystals such as TbVO_4 ⁵ and Nb_3Sn ,⁶ the transition is known to take place primarily as a result of the Jahn-Teller instability; and because of the coupling between such mechanism and strain, the softening of the acoustic phonon is induced (that is, not "proper ferroelastic"). In some crystals such as TeO_2 ,⁷ PrAlO_3 ,⁸ and $\text{KH}_3(\text{SeO}_3)_2$ ⁹ it has been reported that the homogeneous strain is the sole order parameter for the transition. On the other hand, in the piezoelectric crystals such as the LAT under study here, the distinction between whether it is "proper ferroelastic" or not is very clear—constant

χ^x and vanishing C^P constitute the sufficient conditions for the "proper ferroelastic" transition. This result and its implication do not appear to have been emphasized earlier.

One of the authors (M.U.) is grateful to Professor K. Kohn for his continual guidance and encouragements.

¹J. D. Axe, B. Doner, and G. Shirane, *Phys. Rev. Lett.* **26**, 519 (1971).

²M. Maeda, I. Suzuki, and R. Abe, *J. Phys. Soc. Jpn.* **39**, 1319 (1975).

³E. M. Brody and H. Z. Cummins, *Phys. Rev. Lett.* **21**, 1263 (1968).

⁴A full description of the Brillouin scattering experiments on this crystal will be published elsewhere; M. Udagawa, K. Kohn, and T. Nakamura, to be published.

⁵J. R. Sandercock, S. B. Palmer, R. J. Elliott, W. Hayes, S. R. P. Smith, and A. P. Young, *J. Phys. C* **5**, 3216 (1972).

⁶W. Rehwald, *Adv. Phys.* **22**, 721 (1973).

⁷P. S. Peercy and I. J. Fritz, *Phys. Rev. Lett.* **32**, 466 (1974).

⁸P. A. Fleury, P. D. Lazay, and L. G. Van Uitert, *Phys. Rev. Lett.* **33**, 492 (1974).

⁹N. P. Ivanov, L. A. Shuvalov, G. Schmidt, and E. Shtol'p, *Izv. Akad. Nauk SSSR, Ser. Fiz.* **39**, 933 (1975); N. P. Ivanov and L. A. Shuvalov, *Izv. Akad. Nauk SSSR, Ser. Fiz.* **41**, 656 (1977); Y. Makita, F. Sakurai, T. Osaka, and I. Tatsuzaki, *J. Phys. Soc. Jpn.* **42**, 518 (1977).

Quadrupole Influence on the Dipolar-Field Width for a Single Interstitial in a Metal Crystal

O. Hartmann

Institute of Physics, University of Uppsala, Sweden, and CERN, Geneva, Switzerland

(Received 23 May 1977)

The dipolar broadening of the magnetic field sensed by an interstitial impurity in a rigid lattice is calculated with the electric-field gradient set up by the impurity taken into account. This is shown to give a strong dependence of the dipolar width on the applied magnetic field. The theory is especially applicable to the linewidth of precessing muons in metals.

The broadening, due to dipolar coupling, of magnetic resonance lines of nuclear spins I in solids was derived by Van Vleck¹ to be

$$\overline{\Delta\omega_I^2} = \frac{3}{4}\gamma_I^4\hbar^2 I(I+1) \sum \frac{(3\cos^2\theta - 1)^2}{\gamma^6} \quad (1)$$

for the broadening due to like spins, and

$$\overline{\Delta\omega_I^2} = \frac{1}{3}\gamma_I^2\gamma_S^2\hbar^2 S(S+1) \sum \frac{(3\cos^2\theta - 1)^2}{\gamma^6} \quad (2)$$

for the broadening due to unlike spins, i.e., gyromagnetic ratios $\gamma_I \neq \gamma_S$. The equations are valid if the spins are subject to a static magnetic field $B_0 = B_z$ substantially larger than the dipolar fields, which are typically of the order of 1 G for nuclear spins in solids.

In Eq. (2), spin-flip terms of the type I_+S_- are absent, and it can be considered as the random sum of the dipolar fields from all the spins S at

the site of spin I :

$$M_2 = \overline{\Delta B_z^2} = \frac{1}{3} \gamma_S^2 \hbar^2 S(S+1) \sum \frac{(3 \cos^2 \theta - 1)^2}{r^6}, \quad (3)$$

where ΔB_z is the contribution from each spins S to the field along the external field \vec{B}_0 , \vec{r} is the vector from spin S to spin I , and θ the angle between \vec{r} and \vec{B}_0 . M_2 is the second moment of the field distribution. In a single crystal the sum in Eq. (3) will depend on the orientation of the crystal with respect to the external magnetic field \vec{B}_0 .

If Eq. (3) is used to calculate the field distribution sensed by an interstitial in a metal, e.g., a positive muon, certain care must be taken. The muon acts as a charged impurity in the lattice and creates an electric-field gradient at the nearby host nuclei. If these nuclei possess a quadrupole moment, then the direction of the magnetic field \vec{B}_0 is no longer a unique quantization axis. In these circumstances Eq. (3) is no longer valid, and the orientational dependence of the dipolar width is drastically changed. In this case the dipolar fields from the lattice nuclear spins S at the position of the interstitial spin I have to be calculated with the spins S being subject to a combined electric and magnetic interaction.

The general behavior of the nuclear spins S under the influence of a static magnetic field \vec{B}_0 and an electric-field gradient $V_{z'z'}$, in general not parallel to \vec{B}_0 , can be calculated by transforming the electric interaction to the coordinate system defined by \vec{B}_0 .² The diagonalization of the resultant Hamiltonian matrix of order $2S+1$ gives the energies E_k and eigenfunctions $\varphi_k = \sum c_m u_m$ for the stationary states, where the basic functions u_m represent the $(2S+1)$ m states for spin S . Alternatively, the magnetic interaction can be trans-

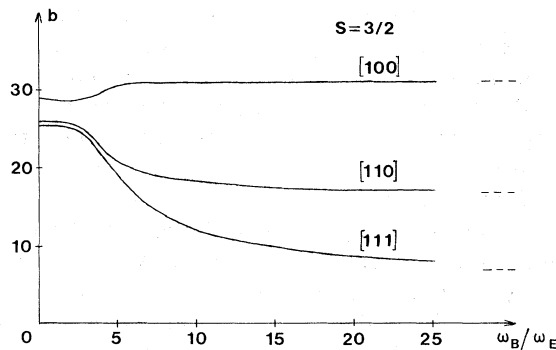


FIG. 1. Calculated linewidths b in fcc structure, octahedral sites, as a function of the relative interaction strength ω_B/ω_E for different orientations of the external field \vec{B}_0 . Broken lines to the right indicate b values in the limit of large ω_B .

formed.³ The components of the magnetic moment of spin S are obtained from the expectation values of the spin operators, i.e., $M_z = \gamma_S \hbar \langle \psi | S_z \times | \psi \rangle$ with $\psi = \sum_k \varphi_k$.

(a) $V_{z'z'} = 0$.—The basic functions u_m are also eigenfunctions, and the spin S will have a static z component in each of the $2S+1$ eigenstates, i.e.,

$$\langle S_z \rangle_m = m, \quad (4)$$

while the components in the x - y plane oscillate with the Larmor frequency so that

$$\langle S_x \rangle = \sum c_i^* c_i' \langle m | S_x | m' \rangle \exp[-(i/\hbar)(E_{m'} - E_m)t]. \quad (5)$$

Oscillating components from Eq. (5) cannot influence spin I with its different Larmor frequency, but the static z components of the magnetic moment give rise to a dipolar field at the site of spin I ,

$$\Delta B_z = \gamma_S \hbar \langle S_z \rangle \frac{3 \cos^2 \theta - 1}{r^3}. \quad (6)$$

By noting that

$$\overline{\langle S_z \rangle^2} = \frac{1}{3} S(S+1),$$

we obtain the random contribution from spin S ,

$$\overline{\Delta B_z^2} = \frac{1}{3} \gamma_S^2 \hbar^2 S(S+1) \frac{(3 \cos^2 \theta - 1)^2}{r^6}. \quad (7)$$

(b) $V_{z'z'}$, making an angle θ with \vec{B}_0 .—We consider now the case where the electric-field gradient $V_{z'z'}$, created by the interstitial is radially directed and axially symmetric. The stationary states of the lattice nuclei S described by the eigenvectors $\varphi_k = \sum c_m u_m$ now have static z components given by

$$\langle S_z \rangle_k^{\text{stat}} = \sum c_i^* c_i m_i, \quad (8)$$

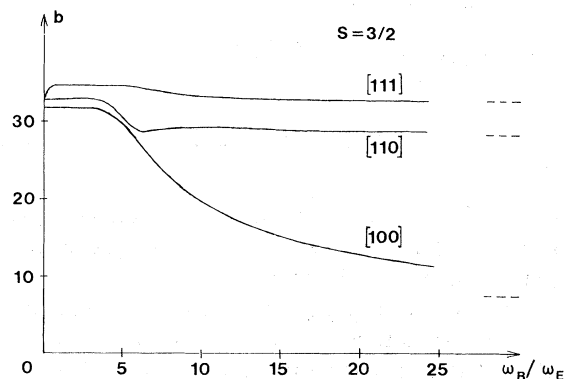


FIG. 2. Calculated linewidths b as in Fig. 1 for fcc structure, tetrahedral sites.

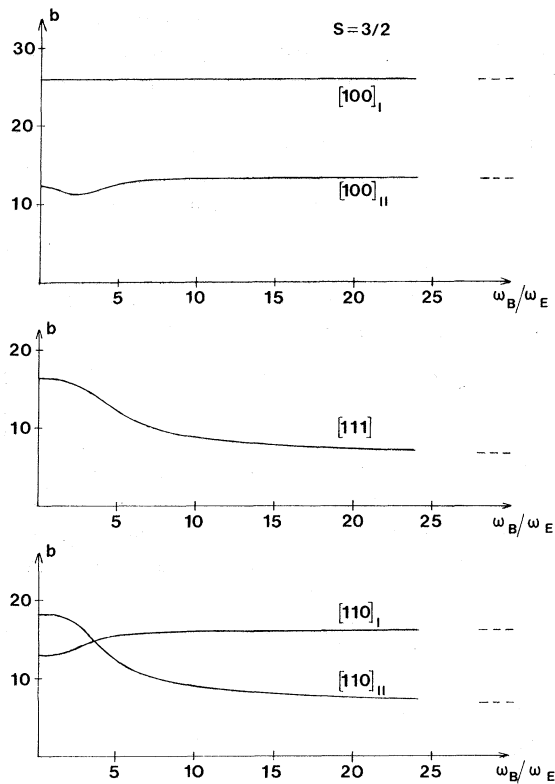


FIG. 3. Calculated linewidths b as in Fig. 1 for bcc structure, octahedral sites.

but also static x components,

$$\langle S_x \rangle_k^{\text{stat}} = \sum c_i^* c_j \langle u_i | S_x | u_j \rangle, \quad (9)$$

due to the mixture of m states in each eigenstate. There will also be a number of oscillating x and z components containing $\exp[-(i/\hbar)(E_{k'} - E_k)t]$. The fluctuating fields can be neglected as long as they do not coincide with the Larmor frequency of spin I , and one will have a resultant static contribution to the field:

$$\Delta B_z = \gamma_S \hbar \langle S_z \rangle_k^{\text{stat}} \frac{3 \cos^2 \theta - 1}{r^3} + \gamma_S \hbar \langle S_x \rangle_k^{\text{stat}} \frac{3 \sin \theta \cos \theta}{r^3}, \quad (10)$$

with $\langle S_z \rangle_k^{\text{stat}}$ and $\langle S_x \rangle_k^{\text{stat}}$ for each eigenstate given by Eqs. (8) and (9), and the x axis chosen in the plane containing \vec{r} and \vec{B}_0 .

The dipolar broadening at interstitial sites in fcc and bcc structures have been calculated as a function of the relative interaction strength $y = \omega_B/\omega_E$; ω_B is the Larmor frequency of the lattice nuclei determined by $\omega_B = \gamma_S B_0$, and ω_E the

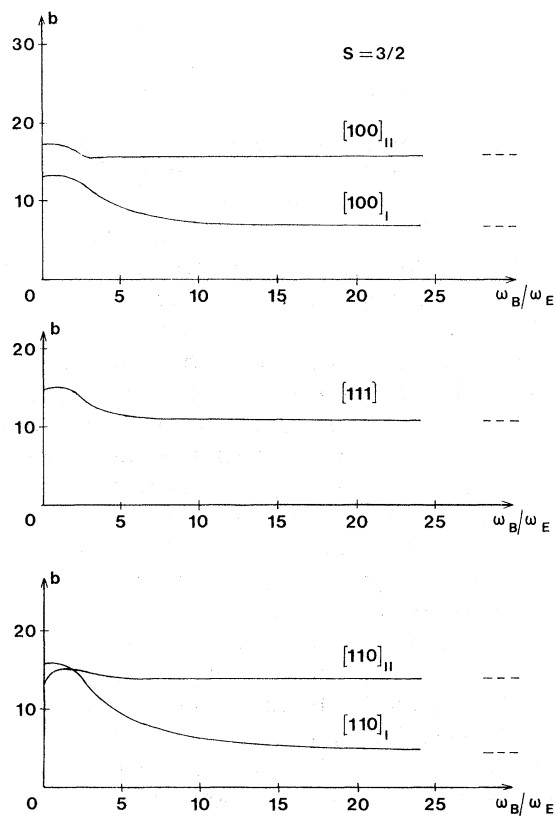


FIG. 4. Calculated linewidths b as in Fig. 1 for bcc structure, tetrahedral sites.

electric interaction frequency given by $\omega_E = (eQ/\hbar)\{V_{z'z'}/[4S(2S-1)]\}$. The parameter b shown in Figs. 1-5 is the rms sum of the contributions in Eq. (10) with $\Delta B_z^2 = b^2 \gamma_S^2 \hbar^2/a^6$, where a is the lattice constant. In general, about seventy lattice points around the interstitial were included.

The field gradient has been assumed to be radially directed from the interstitial and to decrease as r^3 . This choice is not critical as the major part of the sums in Eq. (10) arises from the nearest neighbors. The scale has been chosen such that the parameter $y = \omega_B/\omega_E$ is the interaction strength at the distance $r = \frac{1}{2}a$ from the interstitial site.

The derivation assumes that the frequencies of the oscillating components of the dipolar fields are separated from the interstitial's Larmor frequency; in the opposite case, certain resonance phenomena (spin flips) could occur. For the case of muons in copper $\gamma_\mu \approx 12\gamma_{Cu}$, and the distance of the nearest neighbor is $r = \frac{1}{2}a$ (octahedral sites). The curves in Fig. 1 should then be valid for $\omega_B/\omega_E \geq 0.5$.

Figures 3 and 4 show the situation for bcc

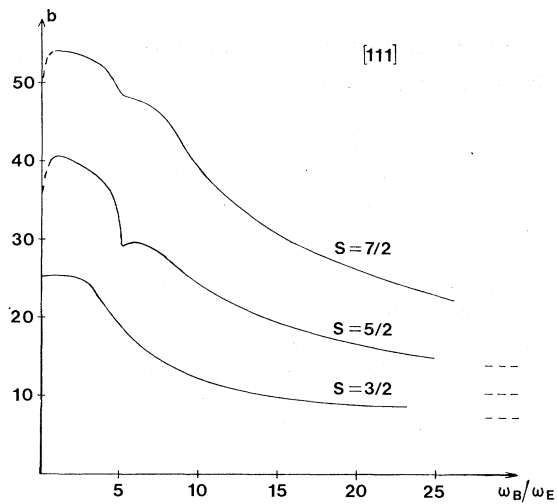


FIG. 5. Calculated linewidths b as in Fig. 1 for fcc structure, octahedral sites, for different values of spin S .

structures. With the field \vec{B}_0 along the [100] or [110] direction, two inequivalent positions exist both in the tetrahedral and octahedral sites. Of these positions, one kind is twice as common as the other, and is indicated by II in the figures.

The interstitial sites in the bcc structure do not have cubic symmetry. This is easily seen for the octahedral positions which have two next neighbors at distance $a/2$ and four at $2^{1/2}a$. The dipolar linewidth is the sum of contributions along the direction given by the magnetic field \vec{B}_0 , and therefore depends on how the noncubic site is oriented with respect to \vec{B}_0 . A field direction like, e.g., [210] results in three different dipolar widths, which for [100] and [110] degenerate into two dipolar widths, and for [111] into one single dipolar width. This inequivalency among the interstitial sites does not occur for

the fcc structure, where both the octahedral and tetrahedral sites have cubic symmetry.

Figure 5 shows the dependence of the line broadening on the spin value S for fcc octahedral positions, in the [111] direction. The general shape of the dependence on ω_B/ω_E is seen to be similar to the different spin values.

The linewidths shown in Figs. 1–5 are what would be observed in a muon-precession experiment at different fields \vec{B}_0 , assuming that the muon creates a radially directed electric-field gradient. Strong effects from field gradients created by impurities (substitutional) have been seen by NMR methods in copper and aluminum.^{4,5} In fact, the presence of electric-field gradients explains the experimental results on positive muon precession in copper, where different crystal orientations give almost equal linewidths $\sigma = 2^{1/2}\gamma_\mu \Delta B$ at low fields B_0 ,^{6,7} and where the linewidth dependence at higher fields⁷ shows a behavior very similar to the curves in Fig. 1.

The author is much indebted to his muon-spin-rotation collaborators L. O. Norlin, E. Karlsson, M. Borghini, T. Niinikoski, and K. Pernestål for numerous discussions about electric-field gradients, and to Dr. A. Schenck for communicating experimental results prior to publication.

¹J. H. Van Vleck, Phys. Rev. **74**, 1168 (1948).

²E. Matthias *et al.*, Phys. Rev. **125**, 261 (1961).

³L. Boström *et al.*, Phys. Scr. **2**, 65 (1970).

⁴J. Stiles and D. L. Williams, J. Phys. F **4**, 2297 (1974).

⁵B. L. Jensen *et al.*, J. Phys. F **2**, 169 (1971).

⁶O. Hartman *et al.*, Phys. Lett. **61A**, 141 (1977).

⁷M. Camani *et al.*, following Letter. [Phys. Rev. Lett. **39**, 836 (1977)].